ELSEVIER

Journal of Organometallic Chemistry 541 (1997) 143–155

Journal of Organometallic Chemistry

Insertion of iridium into C–H and C–S bonds of 2,5-dimethylthiophene, 2-methylbenzothiophene and 4,6-dimethyldibenzothiophene [1]

Claudio Bianchini *, Juan A. Casares [2], Dante Masi, Andrea Meli, Wolfgang Pohl, Francesco Vizza

Istituto per lo Studio della Stereochimica ed Energetica dei Composti di Coordinazione, CNR, Via J. Nardi 39, 50132 Firenze, Italy

Received 30 October 1996; accepted 15 December 1996

Abstract

C–H insertion thienyl products are selectively formed at early times of the interaction of the unsaturated 16e$^-$ fragment [(triphos)IrH] with 2,5-dimethylthiophene (Me_2T), 2-methylbenzothiophene (MeBT) and 4,6-dimethyldibenzothiophene (Me_2DBT) [triphos = $MeC(CH_2PPh_2)_3$]. C–S insertion to give six-membered metallathiacycle products occurs as a thermal step only for Me_2T and MeBT. The C–S insertion products are isolated as both kinetic and thermodynamic stereoisomers. The thermodynamic C–S insertion product of MeBT, endo-[(triphos)Ir(η^3-*S*,*C*,*C*-S(C_6H_4)CH=C(Me)H)], has been characterized by X-ray diffraction studies. © 1997 Elsevier Science S.A.

Keywords: Hydrodesulfurization; C–H activation; C–S activation; Thiophenes; Iridium

1. Introduction

Despite the fact that alkyl-substituted thiophenes largely prevail over their unsubstituted parents in crude oil as well as in cracking naphthas [1], most of the homogeneous studies of the hydrodesulfurization (HDS) process, particularly as regards the C–S insertion step, are concerned with the model compounds thiophene (T), benzo[*b*]thiophene (BT), and dibenzo[*b*,*d*]thiophene (DBT) [2,3]. The principal reason for the scarcity of reports on the cleavage of polyalkylated thiophenes by soluble metal complexes is given by the importance of steric factors in controlling the C–S insertion step [2–9]. Unlike heterogeneous catalysts, the metal centers in the complexes of current use in HDS modeling studies are sterically crowded and may decompose under the drastic conditions required to overcome the steric barrier to C–S insertion. This occurs particularly for thiophenes and fused-ring thiophenes bearing alkyl substituents proximal to the sulfur atom as it is agreed that S-bound thiophene complexes are the immediate precursors to C–S insertion [6,9]. Indeed, very few metal systems are known to cleave polyalkylated thiophenes by simple thermolysis. The 16-electron fragment [(C_5Me_5)Rh(PMe_3)] [6,7] and the cluster $Fe_3(CO)_{12}$ [10] bring about the C–S scission of 2,5-dimethylthiophene (Me_2T), while the opening of 2-methylbenzo[*b*]thiophene (MeBT) has uniquely been achieved by means of [(C_5Me_5)Rh(PMe_3)] [8]. The latter metal fragment also inserts into the C–S bond in mono-, di- and trimethyl substituted dibenzo[*b*,*d*]thiophenes as well as benzo[*b*]naphtho[*d*]thiophenes [9]. In all cases, the regioselectivity of the C–S insertion is driven primarily by steric factors with a small electronic contribution. No example of C–S bond cleavage of 4,6-dimethyldibenzo[*b*,*d*]thiophene (Me_2DBT) has ever been reported.

A particular type of alternative C–S insertion involves the reaction of either η^5 or η^4-thiophene complexes with bases [11–13] or, more rarely, with electrophiles [14,15]. These bonding modes are less sterically demanding than η^1-*S*-coordination and thus allow even the cleavage of tetramethylthiophene [12,13,15].

As is shown in this work, transition metal complexes stabilized by the tripodal ligand $MeC(CH_2PPh_2)_3$ (tri-

* Corresponding author.

[1] Dedicated to Professor Gottfried Huttner on the occasion of his 60th birthday.

[2] Present address: Departamento de Química Inorganica, Universidad de Valladolid, Spain.

0022-328X/97/$17.00 © 1997 Elsevier Science S.A. All rights reserved.
PII S0022-328X(97)00046-6

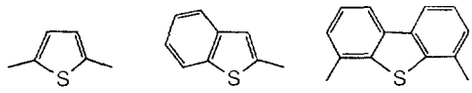

Me_2T MeBT Me_2DBT

Scheme 1.

phos) may provide some breakthroughs into the activation of encumbered thiophenes. Due to the 'polydentate effect' [16] as well as the exclusive *fac* binding mode of the tripod, triphos forms both thermally robust and highly energetic metal fragments, which are capable of cleaving monosubstituted thiophenes [4], BT [17–19], DBT [3,20], and fused-ring thiophenes higher than DBT such as dinaphtho[2.1-*b*:1′.2′-*d*]thiophene (DNT) [21].

The excellent thermal stability has also allowed the [(triphos)MH] (M = Rh, Ir) moieties to be successfully employed as catalysts for the homogeneous hydrogenolysis of T, BT, DBT and DNT to the corresponding thiols under reaction conditions that common metal fragments do not generally tolerate (160–200 °C, 15–60 atm H_2) [3,21,22].

Studies of the interaction between the fragment [(triphos)IrH] and Me_2T, MeBT and Me_2DBT (Scheme 1) are described here and the evidence for insertion of iridium into a C–S bond of the first two substrates is reported.

2. Experimental section

2.1. General procedure

All reactions and manipulations were routinely performed under a nitrogen atmosphere by using standard Schlenk techniques. High-temperature reactions were performed with a stainless steel Parr 4565 reactor equipped with a Parr 4842 temperature and pressure controller. Tetrahydrofuran (THF) was distilled from $LiAlH_4$, stored over molecular sieves and purged with nitrogen prior to use. 2,5-Dimethylthiophene (98.5%, Me_2T) was purchased from Aldrich and used without further purification. All other chemicals were commercial products and were used as received without further purification. 2-Methylbenzo[*b*]thiophene [8] (MeBT), 4,6-dimethyldibenzo[*b*,*d*]thiophene [23] (Me_2DBT), and [(triphos)Ir(H)$_2$(C_2H_5)] [24] were prepared as previously described. Deuterated solvents for NMR measurements were dried over molecular sieves. ^1H, $^{13}C\{^1H\}$, and $^{31}P\{^1H\}$ NMR spectra were obtained on either a Bruker ACP 200 (200.13, 50.32, and 81.01 MHz respectively) or a Varian VXR 300 (299.94, 75.43, and 121.42 MHz respectively) spectrometer. All chemical shifts are reported in ppm (δ) relative to tetramethylsilane, referenced to the chemical shifts of residual solvent resonances (^1H, ^{13}C) or 85% H_3PO_4 (^{31}P). Broad band and selective $^1H\{^{31}P\}$ NMR experiments were carried out on the Bruker ACP 200 instrument equipped with a 5 mm inverse probe and a BFX-5 amplifier device. ^{13}C-DEPT, $^1H,^{13}C$ 2D-HETCOR and $^1H,^1H$ 2D-COSY NMR experiments were conducted on the Bruker ACP 200 spectrometer. For selected compounds, the ^1H and $^{31}P\{^1H\}$ NMR spectra were recorded at 500.13 and 202.45 MHz respectively on a Bruker Avance DRX-500 spectrometer equipped with a variable temperature control unit accurate to ± 0.1 °C. The assignments of the signals were obtained from ^1H homonuclear decoupling experiments and proton detected $^1H,^{31}P$ correlations using degassed nonspinning samples. J(HH) and J(HP) coupling constants were obtained from $^1H\{^1H\}$ and $^1H\{^{31}P\}$ decoupling experiments. 2D NMR spectra were recorded using pulse sequences suitable for phase-sensitive representations using TPPI. The $^1H,^{31}P$ correlations [25] were recorded using the standard HMQC sequence with no decoupling during acquisition, 256 increments of size 2 K (with 8 scans each) were collected covering the full range in both dimensions (ca. 5000 Hz in F_2 and ca. 6500 Hz in F_1) with a relaxation delay of 1.5 s. The ^1H 2D-NOESY experiments [26] were recorded with 1024 increments of size 2 K (with 8 scans each) covering the full range (ca. 5000 Hz) in both dimensions and using a mixing time of 0.8 s. Infrared spectra were recorded on a Perkin–Elmer 1600 Series FTIR spectrophotometer using samples mulled in Nujol between KBr plates.

2.2. Reaction of [(triphos)Ir(H)$_2$(C_2H_5)] (1) with MeBT

2.2.1. NMR experiment

A sample of **1** (30 mg, 0.035 mmol) together with a 5-fold excess of MeBT (26 mg, 0.175 mmol) was dissolved in THF-d_8 (0.8 ml) and then transferred into a 5 mm NMR tube under nitrogen. After two freeze/pump/thaw cycles at −196 °C, the tube was flame-sealed and then placed into an oil-bath preheated to 70 °C. After 3 h, the tube was cooled to room temperature and $^{31}P\{^1H\}$ and ^1H NMR spectra were recorded at room temperature.

In addition to the starting complex **1** (10%), the C–H bond activation product [(triphos)Ir(H)$_2$(3-MeBTyl)] (**2**) (MeBTyl = 2-methylbenzo[*b*]thienyl) and the C–S insertion product *exo*-[(triphos)Ir(η^3-*S*,*C*,*C*-S(C_6H_4)CH=C(H)Me)] (**3k**, see below) were observed in a ca. 1:1 ratio (^{31}P NMR integration). Compound **2** was identified by comparison of its $^{31}P\{^1H\}$ and ^1H NMR spectra to those of related benzothienyl complexes [17] [$^{31}P\{^1H\}$ NMR: AM_2 spin system, δ −10.2 (t, $J(P_AP_M)$ = 14.9 Hz, P_A), −19.1 (d, P_M). ^1H NMR: δ −8.34, second order doublet of multiplets, AA′XX′Y spin system, $|J(HP_M) + J(HP_{M'})|$ = 123.1 Hz, $J(HP_A)$ = 13.0 Hz, Ir–H]. The reaction mixture was further kept

at 70 °C for 24 h. Within this time, $^{31}P\{^1H\}$ and ^1H NMR spectra, recorded every 2 h, showed both the disappearance of **1** and the quantitative, although slow, conversion of **2** to **3k**. Heating the NMR tube sequentially to 90, 110 and 130 °C caused no transformation of **3k**. Rearrangement of **3k** to its stereoisomer *endo*-[(triphos)Ir(η^3-*S,C,C*-S(C_6H_4)CH=C(Me)H)] (**3t**, see below) began to occur only at 140 °C (6% after 4 h). The transformation of **3k** into **3t** is much faster at 160 °C: 50 and 100% conversion after 4 and 36 h respectively. In an attempt to obtain mechanistic information on the conversion of **2** to **3k**, a sealed NMR tube containing a benzene-d_6 solution of a 1:1 mixture of **2** and **3k** was heated at 110 °C. Transformation of **2** to **3k** occurred in a selective manner (no trace of benzene activation products was observed).

2.2.2. Synthesis of *exo*-[(triphos)Ir(η^3-*S,C,C*-S(C_6H_4)CH=C(H)Me)] (3k)

A Parr reactor was charged with a solid sample of **1** (0.48 g, 0.57 mmol) and with a solution of MeBT (0.42 g, 2.85 mmol) in THF (50 ml) under nitrogen at room temperature and then heated to 120 °C. After 5 h, the reactor was cooled to room temperature and the contents were transferred into a Schlenk-type flask and then concentrated to ca. 10 ml under vacuum. Addition of ethanol (30 ml), followed by partial evaporation of the solvents under a steady stream of nitrogen, led to the precipitation of **3k** as yellow crystals, which were collected by filtration and washed with *n*-pentane; yield 90%. Anal. Calc. (Found) for $C_{50}H_{48}IrP_3S$: C, 62.16 (61.98); H, 5.01 (4.99); Ir, 19.90 (19.63). $^{31}P\{^1H\}$ NMR (THF-d_8, 20 °C, 81.01 MHz) AMQ spin system, δ −13.9 (t, $J(P_AP_M)$ = 19.5 Hz, $J(P_AP_Q)$ = 17.6 Hz, P_A), −27.1 (dd, $J(P_MP_Q)$ = 36.2 Hz, P_M), −36.1 (dd, P_Q). ^1H NMR (CD_2Cl_2, 20 °C, 200.13 MHz) δ 3.54 (m, H_2), 2.92 (m, H_3), 1.08 (dd, $J(MeH_2)$ = 6.7 Hz, $J(MeP)$ = 9.4 Hz, Me). Broad band $^1H\{^{31}P\}$ NMR (CD_2Cl_2, 20 °C, 200.13 MHz) δ 3.54 (dq, $J(H_2H_3)$ = 8.4 Hz, $J(H_2Me)$ = 6.7 Hz, H_2), 2.92 (d, H_3), 1.08 (d, Me). $^{13}C\{^1H\}$ NMR (THF-d_8, 20 °C, 50.32 MHz) δ 54.8 (dd, $J(CP)$ = 36.3, 8.1 Hz, C_3), 34.0 (dd, $J(CP)$ = 52.1, 7.2 Hz, C_2), 23.2 (s, Me).

2.2.3. Synthesis of *endo*-[(triphos)Ir(η^3-*S,C,C*-S(C_6H_4)CH=C(Me)H)] (3t)

A Parr reactor was charged with a solid sample of **1** (0.48 g, 0.57 mmol) and with a solution of MeBT (0.42 g, 2.85 mmol) in THF (50 ml) under nitrogen at room temperature and then heated to 120 °C. After 5 h, the temperature was raised to 160 °C. After 48 h, the reactor was cooled to room temperature and the contents were transferred into a Schlenk-type flask and concentrated to ca. 10 ml under vacuum. Addition of ethanol (30 ml), followed by partial evaporation of the solvents under a steady stream of nitrogen, led to the precipitation of **3t** as yellow crystals, which were collected by filtration and washed with *n*-pentane; yield 80%. Anal. Calc. (Found) for $C_{50}H_{48}IrP_3S$: C, 62.16 (62.03); H, 5.01 (4.86); Ir, 19.90 (19.71). $^{31}P\{^1H\}$ NMR (THF-d_8, 20 °C, 81.01 MHz) AMQ spin system, δ −8.6 (dd, $J(P_AP_M)$ = 23.8 Hz, $J(P_AP_Q)$ = 13.3 Hz, P_A), −31.6 (dd, $J(P_MP_Q)$ = 33.9 Hz, P_M), −37.0 (dd, P_Q). ^1H NMR (CD_2Cl_2, 20 °C, 200.13 MHz) δ 3.02 (m, H_3), 2.2 (masked by three aliphatic resonances of triphos, the chemical shift was determined by 2D-COSY, H_2), 1.80 (dd, $J(MeH_2)$ = 6.4 Hz, $J(Me_P)$ = 9.3 Hz, Me). Broad band $^1H\{^{31}P\}$ NMR (CD_2Cl_2, 20 °C, 200.13 MHz) δ 3.02 (d, $J(H_3H_2)$ = 8.5 Hz, H_3), 2.2 (masked, H_2), 1.80 (d, $J(MeH_2)$ = 6.4 Hz, Me). $^{13}C\{^1H\}$ NMR (THF-d_8, 20 °C, 50.32 MHz) δ 54.0 (dd, $J(CP)$ = 36.5, 7.2 Hz, C_3), 28.2 (dd, $J(CP)$ = 45.2, 6.4 Hz, C_2), 14.5 (s, Me). Crystals of formula **3t** · 0.5THF, suitable for an X-ray diffraction analysis, were obtained by slow crystallization of **3t** from THF and ethanol under nitrogen at room temperature. Anal. Calc. (Found) for $C_{50}H_{48}IrP_3S \cdot 0.5C_4H_8O$: C, 62.32 (62.11); H, 5.23 (5.13); Ir, 19.18 (18.91).

2.3. Isomerization reaction of 3k to 3t

A Parr reactor was charged with a sample of **3k** (0.10 g, 0.1 mmol) dissolved in THF (or benzene) (20 ml) under nitrogen at room temperature and then heated to 160 °C. After ca. 48 h, the reactor was cooled to room temperature and the contents were transferred into a Schlenk-type flask and concentrated to dryness under vacuum. $^{31}P\{^1H\}$ and ^1H NMR spectra of the residue showed the quantitative conversion of **3k** to **3t**. When the isomerization reaction was carried out in a sealed NMR tube in benzene-d_6 at 160 °C, **3k** was the only product (no trace of benzene activation products was observed). The reaction was also performed in THF-d_8 or benzene-d_6 in the presence of an excess of D_2O, but no incorporation of deuterium in **3t** was observed.

2.4. Reaction of [(triphos)Ir(H)$_2$(C_2H_5)] (1) with Me_2T

2.4.1. NMR experiment

A sample of **1** (30 mg, 0.035 mmol) in THF-d_8 (0.8 ml) was transferred into a 5 mm NMR tube under nitrogen together with a 30-fold excess of Me_2T (120 μl, 1.05 mmol). After two freeze/pump/thaw cycles at −196 °C, the tube was flame-sealed and then placed into an oil-bath preheated to 70 °C. After 3 h, the tube was cooled to room temperature and $^{31}P\{^1H\}$ and ^1H NMR spectra were recorded at room temperature. In addition to the starting complex **1** (34%), the C–H bond activation product [(triphos)Ir(H)$_2$(3-Me_2Tyl)] (**4**) (Me_2Tyl = 2,5-dimethylthienyl) and the C–S insertion product *exo*-[(triphos)Ir(η^3-*S,C,C*-SC(Me)=CHCH=C(H)Me)] (**5k**, see below) were ob-

served in a 2:1 ratio (^{31}P NMR integration). Compound **4** was identified by comparison of its $^{31}P\{^1H\}$ and ^1H NMR spectra to those of related thienyl complexes [17,27] [$^{31}P\{^1H\}$ NMR: AM_2 spin system, δ −9.2 (t, $J(P_AP_M)$ = 14.4 Hz, P_A), −24.2 (d, P_M). ^1H NMR: δ −9.26, second order doublet of multiplets, AA'XX'Y spin system, $|J(HP_M) + J(HP_{M'})|$ = 127.1 Hz, $J(HP_A)$ = 13.2 Hz, Ir–H]. The reaction mixture was further kept at 70 °C for 30 h. Within this time, $^{31}P\{^1H\}$ and ^1H NMR spectra, recorded every 2 h, showed both the gradual disappearance of **1** and the quantitative, although slow, conversion of **4** to **5k**. Heating the reaction mixture sequentially to 90 and 110 °C caused no transformation of **5k**. Upon heating at 120 °C for 1 h, **5k** partially converted to both its stereoisomer *endo*-[(triphos)Ir(η^3-*S,C,C*-SC(Me)=CHCH=C(Me)H)] (**5t**, 15%, see below) and THF activation products (ca. 10%). These include isotopomeric mixtures of [(triphos)Ir(H)$_2$(OC_4D_7)] (**8**) (vide infra), [(triphos)IrH(CO)] [28], [(triphos)IrH$_3$] [28], and other unidentified products [20,29]. By subsequent heating at 140 °C for 8 h, all **5k** converted to **5t**, but the amount of the decomposition products increased to 25%.

2.4.2. *Synthesis of exo-[(triphos)Ir(η^3-S,C,C-SC(Me)=CHCH=C(H)Me)] (5k)*

A Parr reactor was charged with a solid sample of **1** (0.20 g, 0.24 mmol) and with a solution of Me_2T (1.1 ml, 9.6 mmol) in THF (30 ml) under nitrogen at room temperature and then heated at 110 °C for 2 h. The reactor was cooled to room temperature and the contents, transferred into a Schlenk-type flask, were concentrated to ca. 10 ml under vacuum. Portionwise addition of *n*-heptane (30 ml) led to the precipitation of **5k** as yellow crystals, which were collected by filtration and washed with *n*-pentane; yield 90%. Anal. Calc. (Found) for $C_{47}H_{48}IrP_3S$: C, 60.69 (60.53); H, 5.20 (5.19); Ir, 20.67 (20.38). $^{31}P\{^1H\}$ NMR (CD_2Cl_2, 20 °C, 81.01 MHz) AMN spin system, δ −15.2 (t, $J(P_AP_M)$ = 21.2 Hz, $J(P_AP_Q)$ = 15.9 Hz, P_A), −27.1 (dd, $J(P_MP_Q)$ = 35.2 Hz, P_M), −29.1 (dd, P_Q). ^1H NMR (CD_2Cl_2, 20 °C, 200.13 MHz) δ 6.14 (br t, H_4), 3.34 (m, H_2), 2.3 (masked by the aliphatic resonances of triphos, the chemical shift was determined by 2D-COSY, H_3), 1.88 (br s, Me_5), 1.21 (dd, $J(Me_2H_2)$ = 6.8 Hz, $J(Me_2P)$ = 10.1 Hz, Me_2). Broad band $^1H\{^{31}P\}$ NMR (CD_2Cl_2, 20 °C, 200.13 MHz) δ 6.14 (dq, $J(H_4H_3)$ = 4.8 Hz, $J(H_4Me_5)$ = 1.2 Hz, H_4), 3.34 (dq, $J(H_2H_3)$ = 8.0 Hz, $J(H_2Me_2)$ = 6.8 Hz, H_2), 2.3 (masked, H_3), 1.88 (d, Me_5), 1.21 (d, Me_2). $^{13}C\{^1H\}$ NMR (THF-d_8, 20 °C, 50.32 MHz) δ 130 (masked by the phenyl carbon resonances of triphos, the chemical shift was determined by ^1H, ^{13}C 2D-HETCOR, C_4), 49.9 (dd, $J(CP)$ = 32.8, 7.5 Hz, C_3), 35.0 (partially masked by the methylene carbon resonances of triphos, C_2), 23.4 (s, Me_2), 22.2 (d, $J(CP)$ = 5.1 Hz, Me_5).

2.4.3. *Synthesis of endo-[(triphos)Ir(η^3-S,C,C-SC(Me)=CHCH=C(Me)H)] (5t)*

A Parr reactor was charged with a solid sample of **1** (0.20 g, 0.24 mmol) and with a solution of Me_2T (1.1 ml, 9.6 mmol) in THF (10 ml) under nitrogen at room temperature and then heated at 110 °C. After 2 h, the temperature was raised to 140 °C. After 7 h, the reactor was cooled to room temperature and the contents, transferred into a Schlenk-type flask, were concentrated to ca. 10 ml under vacuum. Portionwise addition of *n*-heptane (30 ml) led to the precipitation of a yellow product, which was recrystallized from THF and *n*-heptane to give **5t** in 60% yield. Anal. Calc. (Found) for $C_{47}H_{48}IrP_3S$: C, 60.69 (60.48); H, 5.20 (5.09); Ir, 20.67 (20.33). $^{31}P\{^1H\}$ NMR (CD_2Cl_2, 20 °C, 81.01 MHz) AMN spin system, δ −9.4 (dd, $J(P_AP_M)$ = 23.9 Hz, $J(P_AP_Q)$ = 12.8 Hz, P_A), −32.0 (dd, $J(P_MP_Q)$ = 35.3 Hz, P_M), −33.8 (dd, P_Q). ^1H NMR (CD_2Cl_2, 20 °C, 200.13 MHz) and 5.88 (br t, H_4), 2.4 (masked by the aliphatic resonances of triphos, the chemical shift was determined by 2D-COSY, H_3), 2.10 (br s, Me_5), 2.0 (masked by the aliphatic resonances of triphos, the chemical shift was determined by 2D-COSY, H_2), 1.87 (dd, $J(Me_2H_2)$ = 6.3 Hz, $J(Me_2P)$ = 9.5 Hz, Me_2). Broad band $^1H\{^{31}P\}$ NMR (CD_2Cl_2, 20 °C, 200.13 MHz) δ 5.88 (dq, $J(H_4H_3)$ = 4.6 Hz, $J(H_4Me_5)$ = 1.1 Hz, H_4), 2.4 (masked, H_3), 2.10 (d, Me_5), 2.0 (masked, H_2), 1.87 (d, $J(MeH_2)$ = 6.3 Hz, Me_2). Due to the concomitant overlapping of the H_2 and H_3 with the aliphatic resonances of triphos, $J(H_2H_3)$ could not be evaluated. $^{13}C\{^1H\}$ NMR (THF-d_8, 20 °C, 50.32 MHz) δ 130 (masked by the phenyl carbon resonances of triphos, the chemical shift was determined by ^1H,^{13}C 2D-HETCOR, C_4), 51.3 (dd, $J(CP)$ = 34.8, 6.9 Hz, C_3), 29.6 (dd, $J(CP)$ = 43.5, 9.8 Hz, C_2), 22.7 (d, $J(CP)$ = 4.0 Hz, Me_5), 14.9 (s, Me_2).

2.5. *Isomerization reaction of 5k to 5t*

2.5.1. *THF-d_8*

A 5 mm NMR tube was charged with a sample of **5k** (28 mg, 0.03 mmol) dissolved in THF-d_8 (0.8 ml) under nitrogen at room temperature, flame-sealed and then heated to 140 °C (oil-bath). After 2 h, the tube was cooled to room temperature and $^{31}P\{^1H\}$ and ^1H NMR spectra, recorded at room temperature, showed the presence of the isomer **5t** accompanied by extensive decomposition (ca. 80%).

2.5.2. *Benzene-d_6*

Heating a benzene-d_6 solution of **5k** at 140 °C for 2 h led to the exclusive formation of both [(triphos)Ir(D)$_2$Ph] [29] and **5t** in a ratio of ca. 3:1.

2.6. Reaction of [(triphos)Ir(H)$_2$(C$_2$H$_5$)] (1) with Me$_2$DBT

2.6.1. NMR experiment

A sample of **1** (30 mg, 0.035 mmol) together with a 5-fold excess of Me$_2$DBT (37 mg, 0.175 mmol) was dissolved in THF-d_8 (0.8 ml) and then transferred into a 5 mm NMR tube under nitrogen. After two freeze/pump/thaw cycles at −196 °C, the tube was flame-sealed and then placed into an oil-bath preheated to 70 °C. After 3 h, the tube was cooled to room temperature. ^{31}P{^{1}H} and ^{1}H NMR spectra, recorded at room temperature, showed the complete conversion of **1** to two arene C–H bond activation products of formula [(triphos)Ir(H)$_2$(3-Me$_2$DBTyl)] (**6**, 90%) and [(triphos)Ir(H)$_2$(2-Me$_2$DBTyl)] (**7**, 10%, Me$_2$DBTyl = 4,6-dimethyldibenzo[*b*,*d*]thienyl). These complexes were identified by comparison of their ^{31}P{^{1}H} and ^{1}H NMR spectra to those of related dibenzothienyl complexes [20] [^{31}P{^{1}H} NMR: (**6**) AM$_2$ spin system, δ −9.3 (t, $J(P_AP_M)$ = 14.5 Hz, P_A), −18.27 (d, P_M); (**7**) AM$_2$ spin system, δ −10.1 (t, $J(P_AP_M)$ = 14.5 Hz, P_A), −18.34 (d, P_M). ^{1}H NMR: (**6**) δ −8.40, second order doublet of multiplets, AA′XX′Y spin system, $|J(HP_M) + J(HP_{M'})|$ = 125.3 Hz, $J(HP_A)$ = 13.6 Hz, Ir–H; (**7**) δ −8.22, second order doublet of multiplets, AA′XX′Y spin system, $|J(HP_M) + J(HP_{M'})|$ = 121.6 Hz, $J(HP_A)$ = 13.2 Hz, Ir–H]. The site of C–H activation in **6** and **7** could not be determined experimentally. Further heating of the tube at 70 °C for 3 h did not affect significantly the ratio between **6** and **7**. Only at 90 °C, **6** rapidly converts to **7**. This conversion is accompanied by the formation of the tetrahydrofuranyl complex [(triphos)Ir(H/D)$_2$(OC$_4$D$_7$)] (**8**) originated by C–D bond activation of the solvent. Compound **8** is actually formed as a mixture of different isotopomers due to H/D exchange with moisture or protiated THF. The fully protiated complex **8** was independently prepared by thermolysis of **1** in THF at 100 °C (see below). After 3 and 7 h at 90 °C, compounds **6**, **7** and **8** were detected by ^{31}P{^{1}H} and ^{1}H NMR spectroscopy in ratios of 16:34:50 and 8:21:71 respectively. At 120 °C for 4 h, **6** and **7** rapidly disappeared to give **8** and its thermolysis products [(triphos)IrH(CO)] and [(triphos)IrH$_3$]. At higher temperature (up to 160 °C), several products were formed among which no C–S insertion product of Me$_2$DBT was unambiguously identified.

2.6.2. Synthesis of [(triphos)Ir(H)$_2$(OC$_4$H$_7$)] (8)

A Parr reactor was charged with a solid sample of **1** (0.25 g, 0.3 mmol) in THF (50 ml) under nitrogen at room temperature and then heated at 100 °C for 6 h. The reactor was cooled to room temperature and the contents were transferred into a Schlenk-type flask and then concentrated to ca. 10 ml under vacuum. Portionwise addition of *n*-heptane (30 ml) led to the precipitation of off-white crystals, which were collected by filtration and washed with *n*-pentane (75% yield). Anal. Calc. (Found) for C$_{45}$H$_{48}$IrOP$_3$: C, 60.73 (60.61); H, 5.44 (5.35); Ir, 21.60 (21.00). IR (ν(Ir–H), cm^{-1}) 2050 m. ^{31}P{^{1}H} NMR (CD_2Cl_2, 20 °C, 81.01 MHz) AMQ spin system, δ −9.5 (t, $J(P_AP_M) = J(P_AP_Q) \cong 15.1$ Hz, P_A), −16.8 (t, $J(P_MP_Q) \cong 15.1$ Hz, P_M), −24.4 (t, P_Q). ^{31}P NMR (CD_2Cl_2, 20 °C, 81.01 MHz) δ −9.5 (br, P_A), −16.8 (br d, $J(PM_H) \cong 125$ Hz, P_M), −24.4 (br d, $J(P_QH) \cong 131$ Hz, P_Q). ^{1}H NMR (CD_2Cl_2, 20 °C, 299.94 MHz) δ −9.31 (dtd, $J(HP_M)$ = 130.0 Hz, $J(HP_A) = J(HP_M)$ = 11.9 Hz, $J(H_AH_B)$ = 4.4 Hz, Ir–H_A), −9.42 (dddd, $J(HP_Q)$ = 135.5 Hz, $J(HP_A)$ = 14.2 Hz, $J(HP_M)$ = 10.8 Hz, $J(H_BH_A)$ = 4.4 Hz, Ir–H_B). Broad band ^{1}H{^{31}P} NMR (CD_2Cl_2, 20 °C, 200.13 MHz) δ −9.31 (d, $J(H_AH_B)$ = 4.4 Hz, Ir–H_A), −9.42 (d, Ir–H_B); the two hydrides constitute a slightly second order AB spin system. {Other spectroscopic details of **8** will be published elsewhere, together with a description of its thermolysis to [(triphos)IrH(CO)] and [(triphos)IrH$_3$].}

2.7. X-ray data collection and structure determination of 3t · 0.5THF

Intensities of a yellow crystal were collected on an Enraf–Nonius CAD4 diffractometer. A set of 25 carefully centered reflections having 6° < θ < 8.5° was used to determine the cell constants. Three standard reflec-

Table 1
Crystal and collection data for **3t**·0.5THF

Formula	$C_{52}H_{52}IrO_{0.5}P_3S$
Formula weight (g mol^{-1})	1002.18
Crystal dimensions (mm^3)	0.32 × 0.17 × 0.15
Crystal system	monoclinic
Space group (No.)	$P2_1/n$ (14)
a (Å)	13.194(4)
b (Å)	19.656(4)
c (Å)	18.438(8)
β (deg)	90.98(3)
V (Å^3)	4781(3)
Z	4
F(000)	1944
ρ_{calc} (g cm^{-3})	1.392
Diffractometer	Enraf–Nonius CAD4
Radiation (monochromator)	Mo (Kα), 0.71069 Å (graphite)
Scan rate (deg min^{-1})	5.5
Scan range (deg)	0.8 + 0.35 tan θ
2θ range (deg)	5–45
Data collected	$-14 \le h \le 14$, $0 \le k \le 21$, $0 \le l \le 19$
No. of data collected	6451
No. of unique data	6226
No. of parameters varied	223
μ(Mo Kα) (mm^{-1})	2.967
R_1 [$I > 2\sigma(I)$]	0.0503
Rw_1	0.1269
Goodness of fit on F^2	1.045

Table 2
Selected bond lengths [Å] and angles [deg] for **3t**·0.5THF

Ir(1)–C(6)	2.131(13)
Ir(1)–C(8)	2.141(12)
Ir(1)–P(1)	2.271(3)
Ir(1)–P(3)	2.328(3)
Ir(1)–P(2)	2.333(3)
Ir(1)–S(1)	2.417(3)
S(1)–C(1,7)	1.767(13)
C(6)–C(8)	1.45(2)
C(6)–C(7)	1.53(2)
C(8)–C(2,7)	1.47(2)
C(6)–Ir(1)–C(8)	39.8(5)
C(6)–Ir(1)–P(1)	90.4(4)
C(8)–Ir(1)–P(1)	93.7(3)
C(6)–Ir(1)–P(3)	119.8(4)
C(8)–Ir(1)–P(3)	159.5(3)
P(1)–Ir(1)–P(3)	88.09(12)
C(6)–Ir(1)–P(2)	150.4(4)
C(8)–Ir(1)–P(2)	110.7(3)
P(1)–Ir(1)–P(2)	89.24(12)
P(3)–Ir(1)–P(2)	89.77(12)
C(6)–Ir(1)–S(1)	85.1(4)
C(8)–Ir(1)–S(1)	82.0(3)
P(1)–Ir(1)–S(1)	175.27(12)
P(3)–Ir(1)–S(1)	95.39(12)
P(2)–Ir(1)–S(1)	93.98(12)
C(1,7)–S(1)–Ir(1)	98.3(4)
C(8)–C(6)–C(7)	124.0(12)
C(8)–C(6)–Ir(1)	70.4(7)
C(7)–C(6)–Ir(1)	126.7(10)
C(6)–C(8)–C(2,7)	120.7(12)
C(6)–C(8)–Ir(1)	69.7(7)
C(2,7)–C(8)–Ir(1)	114.0(9)

tions were measured every 2 h for the orientation and the intensity control. During data collection no decay for the specimen was noticed. Intensity data were corrected for Lorentz–polarization effects. Atomic scattering factors were those reported by Cromer and Waber [30] with anomalous dispersion correction taken from Ref. [31]. An empirical absorption correction was applied via ψ scan with transmission factors in the range 71.03–99.96 [32]. The computational work was carried out by intensively using the program SHELXL93 [33]. Crystallographic details are reported in Table 1, selected bond distances and angles in Table 2 and final atomic coordinates with equivalent isotropic parameters in Table 3. Tables of hydrogen atom coordinates and anisotropic displacement parameters and a complete list of bond lengths and angles have been deposited at the Cambridge Crystallographic Data Centre. The structure was solved by direct methods using the SIR92 program [34] and all of the non-hydrogen atoms were found through a series of F_o Fourier maps. A THF solvent molecule was also introduced, although affected by some disorder. All the atoms were treated as carbon and assigned a population factor of 0.5. Hydrogen atoms were introduced at calculated positions at the late stage

Table 3
Atomic coordinates ($\times 10^4$) and equivalent isotropic displacement parameters ($Å^2 \times 10^3$) for **3t**·0.5THF

Atom	x	y	z	U_{eq}
Ir(1)	3682(1)	2235(1)	7247(1)	39(1)
P(1)	4266(2)	2152(2)	6099(2)	41(1)
P(2)	2561(2)	3082(2)	6856(2)	44(1)
P(3)	4916(3)	3060(2)	7469(2)	45(1)
S(1)	3052(3)	2222(2)	8470(2)	54(1)
C(1)	4159(9)	2975(6)	5592(6)	47(3)
C(2)	3261(9)	3800(6)	6455(6)	48(3)
C(3)	5162(9)	3542(7)	6621(6)	54(3)
C(4)	4258(9)	3600(6)	6079(6)	44(3)
C(5)	4502(10)	4193(6)	5576(7)	55(4)
C(6)	4025(10)	1190(7)	7433(7)	53(3)
C(7)	4381(12)	870(7)	8148(8)	73(4)
C(8)	2966(9)	1258(6)	7212(7)	49(3)
C(2,1)	4051(5)	851(4)	5495(4)	54(3)
C(3,1)	3617(7)	357(3)	5049(5)	59(4)
C(4,1)	2824(7)	527(4)	4577(4)	71(4)
C(5,1)	2466(6)	1192(5)	4551(4)	78(5)
C(6,1)	2900(6)	1686(3)	4997(5)	65(4)
C(1,1)	3693(6)	1516(3)	5469(4)	39(3)
C(2,2)	6180(6)	1620(4)	6534(3)	55(3)
C(3,2)	7167(6)	1406(4)	6416(4)	67(4)
C(4,2)	7585(5)	1476(5)	5733(5)	82(5)
C(5,2)	7016(7)	760(5)	5169(4)	78(5)
C(6,2)	6029(6)	1975(4)	5287(4)	55(3)
C(1,2)	5611(5)	1905(4)	5970(4)	42(3)
C(2,3)	1020(7)	3064(4)	7849(5)	56(4)
C(3,3)	368(6)	3330(5)	8362(5)	66(4)
C(4,3)	378(7)	4023(5)	8512(5)	80(5)
C(5,3)	1040(8)	4450(4)	8150(5)	88(5)
C(6,3)	1691(7)	4185(4)	7638(5)	79(5)
C(1,3)	1682(6)	3492(5)	7487(4)	50(3)
C(2,4)	1201(7)	3316(4)	5662(5)	74(4)
C(3,4)	431(7)	3122(5)	5181(5)	90(5)
C(4,4)	49(7)	2464(6)	5201(5)	87(5)
C(5,4)	436(8)	1999(4)	5702(6)	94(6)
C(6,4)	1206(7)	2193(4)	6183(5)	76(4)
C(1,4)	1588(6)	2851(5)	6163(4)	46(3)
C(2,5)	3852(6)	3804(4)	8524(5)	55(4)
C(3,5)	3715(6)	4340(5)	9004(5)	78(5)
C(4,5)	4461(7)	4834(4)	9087(4)	76(4)
C(5,5)	5344(6)	4793(4)	8689(5)	67(4)
C(6,5)	5481(5)	4257(5)	8208(5)	63(4)
C(1,5)	4735(7)	3763(4)	8126(4)	53(3)
C(2,6)	6202(6)	2318(5)	8351(4)	60(4)
C(3,6)	7116(7)	2037(4)	8588(4)	84(5)
C(4,6)	8014(6)	2218(5)	8254(5)	81(5)
C(5,6)	7997(5)	2680(5)	7683(5)	87(5)
C(6,6)	7083(7)	2961(4)	7446(4)	66(4)
C(1,6)	6185(5)	2780(4)	7780(4)	49(3)
C(1,7)	2143(9)	1569(6)	8360(7)	50(3)
C(2,7)	2156(10)	1174(7)	7740(7)	54(3)
C(3,7)	1352(10)	739(7)	7603(7)	61(4)
C(4,7)	536(12)	675(8)	8081(8)	72(4)
C(5,7)	586(12)	1065(8)	8714(8)	73(4)
C(6,7)	1365(11)	1499(7)	8858(8)	68(4)
C(1S)	2509(50)	176(34)	1540(35)	202(27)
C(2S)	3435(48)	486(37)	1376(42)	188(32)
C(3S)	2690(54)	−77(35)	845(35)	209(27)
C(4S)	2905(66)	743(38)	772(42)	202(39)
C(5S)	3198(60)	242(43)	278(37)	200(35)

U_{eq} is defined as one third of the trace of the orthogonalized U_{ij} tensor.

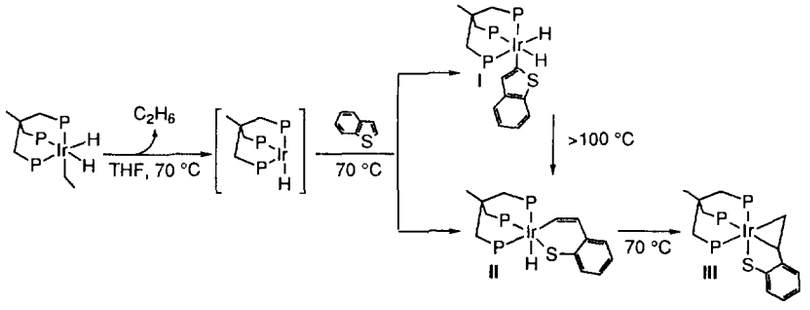

Scheme 2.

of refinement. The latter was done by full-matrix least-squares calculations, initially with isotropic thermal parameters. In the final least-squares cycles, anisotropic thermal parameters were used for the Ir, P, S species and also for the C atoms of the ligand chain. In the final ΔF maps significant peaks were found close to the heavy metal and were considered as ripples of no chemical relevance.

3. Results and discussion

3.1. Reaction of [(triphos)IrH] with 2-methylbenzo[b]thiophene

[(triphos)Ir(H)$_2$(C$_2$H$_5$)] (**1**) is known to reductively eliminate ethane upon thermolysis in refluxing THF [29]. The resulting 16-electron fragment [(triphos)IrH] is capable of oxidatively adding a variety of C–X bonds, including C–H and C–S bonds from T [17,27], BT [17,19] and DBT [20]. In the presence of these substrates, transient [(triphos)IrH] generally shows kinetic preference for C–H bond cleavage to give (thienyl)dihydride complexes, but C–S bond cleavage is thermodynamically favored. In the particular case of BT, both C–H and C–S insertions occur in parallel reactions to give (2-benzothienyl)dihydride (**I**) and (iridathiacyclohexadiene)hydride (**II**) complexes respectively (Scheme 2) [17]. Already at 70 °C, the iridathiacycle compound isomerizes to the 2-vinylthiophenolate complex (**III**), which is also the thermodynamic sink of the thermolysis of the C–H insertion product. From various studies it was concluded that (i) the activation energy for the C–S bond scission reaction (formation of **II**) is lower than that for the C–H bond scission; (ii) the **I** → **III** rearrangement proceeds with no dissociation of BT.

The thermolysis of **1** in THF in the presence of an excess of MeBT proceeds similarly to that with BT (Scheme 3); both C–H and C–S insertion reactions occur to give the 3-methylbenzothienyl dihydride [(triphos)Ir(H)$_2$(3-MeBTyl)] (**2**) (MeBTyl = 2-methylbenzo[*b*]thienyl) and the 2-*n*-propenylthiophenolate complex *exo*-[(triphos)Ir(η^3-*S*,*C*,*C*-S(C$_6$H$_4$)CH=C(H)Me)] (**3k**).

Due to the presence of the methyl substituent in the benzo[*b*]thiophene substrate, C–H insertion selectively occurs at the 3-position, which is the disfavored position for BT where the sulfur atom activates the α-CH bond. Since the spectroscopic characteristics of **2** are quite comparable with those of the analogous BT-derived complex [(triphos)Ir(H)$_2$(2-BTyl)] (BTyl = benzothienyl) [17], a detailed account of the NMR and IR spectra of **2** is not given here. Unlike BT, however, the conversion of the C–H insertion product **2** to the C–S insertion product **3k** already occurs at 70 °C so that after 24 h (NMR experiment) only **3k** is present in the reaction mixture. Moreover, no (iridathiacycloxahediene)hydride intermediate is seen by NMR spectroscopy, which is consistent with a very low energy barrier to hydride migration to the C$_\alpha$ carbon atom of the C–S inserted MeBT molecule. Selective transforma-

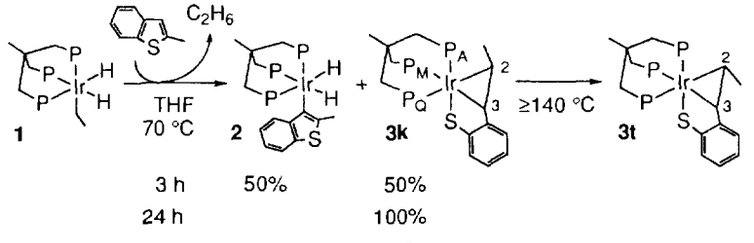

Scheme 3.

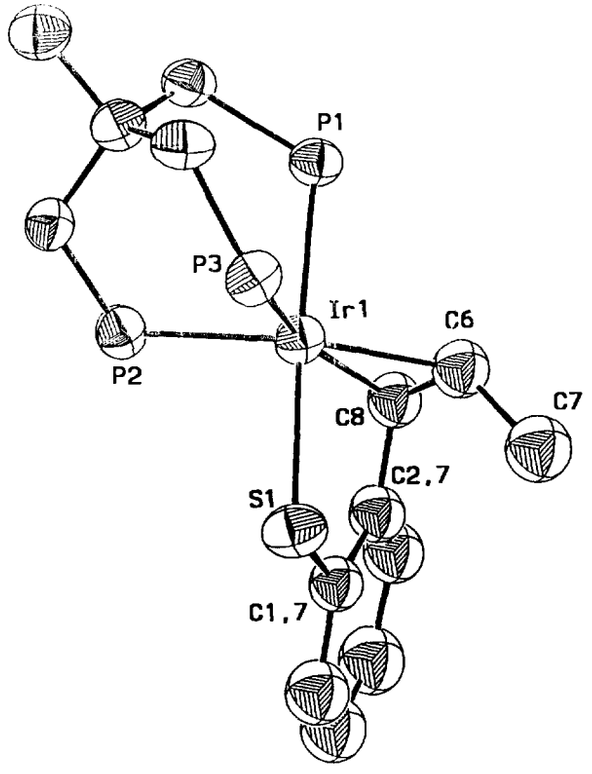

Fig. 1. ORTEP drawing of **3t**·0.5THF. All of the hydrogen atoms and phenyl rings of triphos are omitted for clarity.

tion of **2** into **3k** also occurs in benzene solution, which is consistent with an intramolecular mechanism [17]. A dissociative mechanism like that observed for the conversion of the (dibenzo[*b*,*d*]thienyl)dihydride complexes [(triphos)Ir(H)$_2$(DBTyl)] (DBTyl = 4-, 3- and 2-dibenzothienyl) to the C–S insertion product [(triphos)IrH(η^2-*C*,*S*-DBT)] [20] would have led, in benzene, to the formation of [(triphos)Ir(H)$_2$Ph]. This very stable compound, in fact, always forms whenever transient [(triphos)IrH] is generated in benzene solution (vide infra) [20,29].

Once formed, **3k** is stable in solution up to 130 °C. Above this temperature, **3k** begins to convert to its stereoisomer *endo*-[(triphos)Ir(η^3-*S*,*C*,*C*-S(C$_6$H$_4$)CH=C(H)Me)] (**3t**) (Scheme 3).

In order to isolate both **3k** and **3t** for characterization, conditions were sought under which the selective formation of either compound was optimized. This was accomplished by performing the thermolysis of **1** in autoclaves at 120 °C (**3k**) and 160 °C (**3t**).

Unambiguous identification of **3t** has been provided by an X-ray analysis on a single crystal grown by slow crystallization from THF/ethanol solution. An ORTEP drawing of the complex molecule of **3t** is shown in Fig. 1. Selected bond distances and angles are reported in Table 2.

The structure consists of discrete *endo*-[(triphos)Ir(η^3-*S*,*C*,*C*-S(C$_6$H$_4$)CH=C(H)Me)] molecules and clathrated THF molecules in a 1:0.5 ratio. The coordination geometry around iridium is a distorted octahedron. The phosphorus atoms of triphos occupy three *fac* positions of the coordination polyhedron, the P–Ir–P angles being a bit less than 90°, as usual. The coordination of the metal fragment is completed by a 2-*n*-propenylthiophenolate ligand which uses the sulfur atom, *trans* to P1, and the carbon atoms (C6, C8) of the olefinic moiety. The C6, C8, Ir, P2 and P3 atoms are almost coplanar (±0.035 Å). The nonplanarity of the *n*-propenylthiophenolate ligand may be seen in the 56° C6–C8–C2,7–C1,7 torsion angle. The Ir–(C6–C8) coordination exhibits a C–C distance [1.45(2) Å] that indicates an appreciable amount of metal-to-olefin π-backbonding (metallacyclopropane structure) [27]. A similar structural feature has previously been observed in other C–S insertion products of T and BT with the [(triphos)IrH] fragment [19,27]. The local stereochemistry of the olefinic moiety of the thiolate ligand in **3t** is clearly *Z* (C7–C6–C8–C2,7 torsion angle of 16°), thus the methyl substituent in the olefinic moiety is assigned an *endo* conformation.

The stereochemical rigidity of **3t** in solution allows NMR spectroscopy to show that the solid state structure is maintained also in solution. The ^{31}P{^{1}H} NMR spectrum consists of a temperature-invariant AMQ spin system as expected for the magnetic inequivalence of the three phosphorus atoms. The metallacyclopropane structure of the Ir(C$_2$–C$_3$) coordination is confirmed by the chemical shifts and coupling constants of the two CH groups [C$_3$, δ 54.0, J(CP) = 36.5, 7.2 Hz; C$_2$, δ 28.2, J(CP) = 45.2, 6.4 Hz; H$_3$, δ 3.02, J(H$_3$H$_2$) = 8.5 Hz; H$_2$, δ 2.2] [19].

Besides confirming the structure of **3t**, NMR spectroscopy allows also the identification of the kinetic C–S insertion product **3k** whose ^{31}P{^{1}H} NMR spectrum is quite similar to that of the thermodynamic product **3t** (AMQ pattern) with only minor differences in the chemical shifts. In the ^{1}H NMR spectrum of **3k**, both chemical shifts and coupling constants relative to the MeCH–CH grouping are consistent with an *exo* position of the methyl substituent and, thus, with the *E* configuration of the olefinic moiety. The methyl group, in fact, is shifted upfield (δ 1.08 vs. 1.80 in **3t**) while, most importantly, the H$_3$ proton is now more shielded than the H$_2$ proton (H$_2$, δ 3.54; H$_3$, δ 2.92) [35]. Conclusive experimental evidence of the *E* configuration of the olefinic moiety in **3k** was provided by ^{1}H 2D-NOESY spectroscopy in THF-d_8 after ^{1}H and ^{31}P resonances had been assigned by means of ^{1}H homonuclear decoupling experiments and proton detected ^{1}H,^{31}P correlations. The phosphorus resonances were attributed from the 2D-^{1}H,^{31}P spectrum by the couplings to the protons in *trans* position. In particular, the dd at −36.1 ppm was assigned to the P$_Q$ phosphorus due to the couplings to the H$_2$ proton (J(HP) = 6.3 Hz) and to

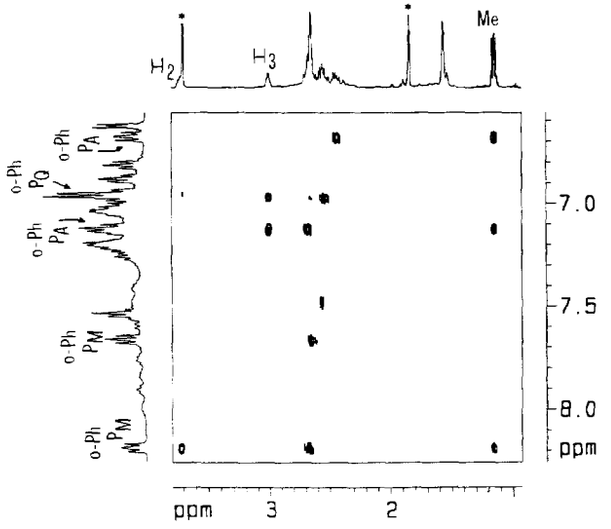

Fig. 2. Section of the ^{1}H 2D-NOESY spectrum of **3k** (500.13 MHz, THF-d_8, 21 °C). All cross-peaks are anti-phased with respect to the diagonal ones; asterisk denotes the residual solvent proton resonances.

the methyl protons (J(HP) = 9.4 Hz), the dd at −27.1 ppm was assigned to the P_M nucleus due to the coupling to the H_3 proton (J(HP) = 3.2 Hz), and the triplet at −13.9 ppm (which shows only a very small coupling to the H_3 proton) was assigned to the P_A phosphorus in apical position. On the basis of these assignments, the ^{1}H resonances of each *ortho*-phenylphosphino proton were readily identified from the ^{1}H,^{31}P correlation. NOEs from these protons to the H_2, H_3 and methyl protons were of crucial importance for establishing the conformation of compound **3k** in solution. A section of the ^{1}H 2D-NOESY spectrum of **3k** is reported in Fig. 2. The crucial NOEs are those between (i) the methyl protons and both couples of P_A *ortho*-phenyl protons, (ii) the H_3 proton and one couple of the P_A *ortho*-phenyl protons. These cross-peaks and the absence of NOE from H_2 to the P_A phenyl protons (this proton shows a strong NOE to the P_M *ortho*-phenyl protons which lies below the Ir–C_2–C_3 plane) unequivocally identify **3k** as the *exo*-isomer.

In search of a mechanism for the rearrangement of **3k** to **3t**, the isomerization reaction was followed by NMR spectroscopy in situ, initially in THF-d_8, then in benzene-d_6. In both solvents, the rearrangement occurs with neither detectable intermediates nor the formation of any isotopomer of the (phenyl)hydride complex [(triphos)Ir(H)$_2$Ph] (see above). These experiments thus suggest that **3k** rearranges to **3t** via an intramolecular mechanism whose steps are still obscure as we observed neither intermediate species nor deuterium incorporation when the reaction was carried out in the presence of excess D_2O.

From a perusal of the solid state structure of **3t**, one may perhaps conclude that the driving force for the isomerization is steric in nature as the methyl group in the *endo* isomer is directed away from the two phenyl substituents on the apical phosphorus, whereas it points to this phosphorus in the *exo* isomer.

Prior to this work, C–S opening of MeBT has uniquely been reported by Jones and coworkers [8]. Like [(triphos)IrH], the fragment [(C_5Me_5)Rh(PMe_3)] employed by Jones yields, at early reaction times, a C–H activation product and a C–S insertion product resulting from insertion of Rh into the C–S bond adjacent to the methyl substituent. Prolonged heating converts this C–S insertion complex to the isomer in which the metal has inserted into the C–S bond adjacent to the aryl group (Scheme 4). The driving force for this intramolecular rearrangement has been proposed to be the formation of a stronger metal–aryl bond as compared to a metal–alkyl.

Intrigued by the possibility of insertion of iridium from [(triphos)IrH] into the C–S bond adjacent to the aryl group of MeBT, **3t** in THF was heated for 24 h at 160 °C in an autoclave. No conversion was observed however.

3.2. Reaction of [(triphos)IrH] with 2,5-dimethylthiophene

Thermolysis of **1** in THF with Me_2T at 70 °C produces the C–H activation complex [(triphos)Ir(H)$_2$(3-Me_2Tyl)] (**4**) (Me_2Tyl = 2,5-dimethylthienyl) and the C–S insertion complex *exo*-[(triphos)Ir(η^3-*S*,*C*,*C*-SC(Me)=CHCH=C(H)Me)] (**5k**). Monitoring the thermolysis reaction by NMR spectroscopy shows that the C–H insertion product disappears upon prolonged heating (30 h), converting to **5k**, which is stable in THF

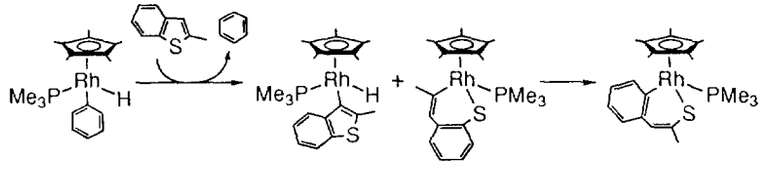

Scheme 4.

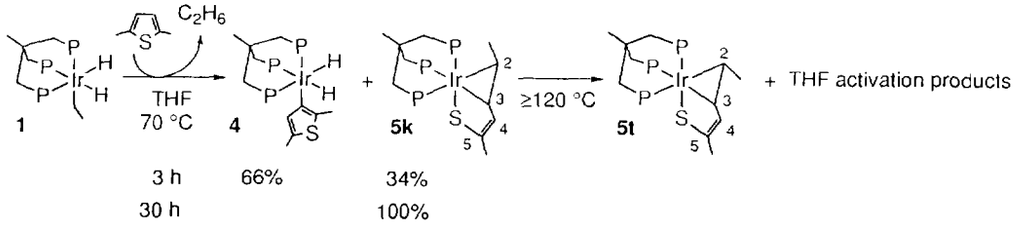

Scheme 5.

solution up to 110 °C. Above this temperature, **5k** is seen to decrease with concomitant formation of a new product that we assign as *endo*-[(triphos)Ir(η³-*S*,*C*,*C*-SC(Me)=CHCH=C(H)Me)] (**5t**) (Scheme 5).

The C–H activation product **4**, even though obtained as a mixture with **5k**, can unequivocally be authenticated through a comparison of its spectroscopic properties with those of the known thienyl complex [(triphos)Ir(H)$_2$(2-Tyl)] [27]. In contrast, identification of the kinetic and thermodynamic C–S insertion products is obtained by NMR spectroscopy on isolated samples prepared in an autoclave. This shows that no terminal hydride is present in both products, while they both contain butadienethiolate ligands. In particular, the close analogies existing between the ^{31}P and ^{1}H NMR spectra of **5k** and **5t** are consistent with two geometric isomers differing in the orientation of the methyl substituent in the distal olefinic end of the butadienethiolate ligand. Both compounds exhibit comparable AMQ ^{31}P patterns, while the trends of the ^{13}C and ^{1}H NMR resonances due to the MeCH–CH moieties are analogous to those observed for the MeBT-derived products **3k** and **3t**. In particular, the methyl resonates at higher field in the *exo* isomer **5k** (δ 1.21 vs. 1.87), while the chemical shifts of H_2 are reversed in the two compounds (**5k**: δ H_2 3.34, δ H_3 2.3; **5t**: δ H_2 2.0, δ H_3 2.4). Moreover, the chemical shifts of the carbon and hydrogen nuclei of the free olefinic moiety are quite similar in the two compounds, confirming that the stereoisomerism is essentially due to the different structure of the bound olefinic end (*E* in **5k**, *Z* in **5t**).

While the overall interaction of transient [(triphos)IrH] with Me_2T is apparently identical with that with MeBT, a difference is seen in the isomerization of the kinetic C–S insertion product to the thermodynamic one. The isomerization of **5k** to **5t**, in fact, is not completely selective as it is invariably accompanied by the concomitant formation of products derived from the activation of the solvent. When isolated **5k** is heated at 140 °C in THF for 2 h, a mixture of products is obtained in which the concentration of **5t** is four times lower than that (overall) of compounds such as [(triphos)IrH(CO)] [28], [(triphos)IrH$_3$] [28], and other THF-activation products (vide infra), which are known to form upon thermolysis of **1** in sole THF at 140 °C [20,29]. A similar situation is observed in benzene as the thermolysis of **3k** at 140 °C produces **5t** and the (phenyl)hydride complex [(triphos)Ir(H)$_2$Ph] in a ca. 1:3 ratio. Only when the thermal isomerization in THF is carried out in the presence of an excess of Me_2T, does the formation of the thermodynamic product **5t** largely prevail over that of the solvent-activation by-products. These experiments and the thermal stability of **5t** in solution at 140 °C, taken together, suggest that **5k** transforms into **5t** by a mechanism which involves the dissociation of Me_2T. Possible steps for the dissociation of Me_2T (determined by GC-MS) are the reverse hydride migration from the C_2 carbon atom to iridium, followed by ring-closure. The latter reaction path has been proved experimentally for DBT [20]. On the other hand, one may not exclude that the thermolysis of **5k** may proceed through two parallel pathways: (i) the intramolecular *Z* to *E* isomerization of the bound double bond of the butadienethiolate ligand, as observed for **3k**; (ii) the dissociation of Me_2T to regenerate [(triphos)IrH], which may react with either the solvent or the thiophene.

Me_2T is one of the most refractory thiophenic molecules to activate by soluble metal complexes [36]. The two methyl substituents enhance the nucleophilic character of the sulfur atom, thus favoring η¹-*S*-coordination [37], but disfavor both C–H and C–S insertion for steric reasons. The negative influence of the methyl groups on C–H insertion may readily be inferred as one considers that η²-*C*,*C*-thiophene coordination, which is believed to precede C–H bond cleavage [6], is sterically disfavored by substituents in the thiophene. As a matter of fact, only one example of η²-*C*,*C*-coordination of Me_2T has been reported, i.e. $[Os(NH_3)_5(2,5\text{-}Me_2T)]^{2+}$ where the supporting metal fragment is not sterically demanding at all [38]. Less intuitive is the role of the two methyl substituents in depressing the tendency for C–S insertion as η¹-*S*-thiophene complexes are believed to be the immediate precursors to C–S bond cleavage [6]. On the other hand, steric effects may clearly be important as one takes into account that the energy barrier to C–S insertion (occurring via a three-centered MC-S transition state [8]) increases with the steric hindrance at the C–S bond.

The fact that the 16-electron fragment [(triphos)IrH] is capable of oxidatively adding both C–H and C–S bonds from Me_2T is in line with the great basicity and

moderate steric hindrance at iridium. These considerations obviously hold also for the activation of MeBT and Me_2DBT and will be further developed in the next section.

3.3. Reaction of [(triphos)IrH] with 4,6-dimethyldibenzo[b,d]thiophene

The steric encumbrance provided by the methyl substituents in the 4- and 6-positions of Me_2DBT, disfavoring η^1-*S* coordination, reasonably accounts for the non-observation of C–S bond cleavage of this thiophene by soluble metal complexes. Some examples of C–S insertion products of either DBT or alkyl-substituted DBTs are known however [7,9,20,39,40]. The methyl substituents in Me_2DBT do not hinder C–H activation pathways; indeed the thermolysis of **1** in THF with Me_2DBT produces, already at 70 °C, the two (dibenzothienyl)dihydride complexes [(triphos)Ir(H)$_2$(3-Me_2DBTyl)] (**6**) and [(triphos)Ir(H)$_2$(2-Me_2DBTyl)] (**7**) (Me_2DBTyl = 4,6-dimethyldibenzo[*b*,*d*]thienyl) in a ca. 9:1 kinetic ratio after 3 h (Scheme 6). Structurally analogous C–H insertion products have been reported to form at early times of the thermolysis of either **1** [20] or [(C_5Me_5)Rh(PMe_3)PhH] [9] in the presence of DBT or substituted DBTs.

Although the site of C–H activation could not be determined experimentally, we tentatively assign **6** as the major kinetic product for the following reasons. Activation of the C–H bond in the 1-position may be excluded on the basis of steric factors. In an eventual 1-DBTyl complex, in fact, the other phenyl ring would be too close to the phenyl substituents on the basal P atoms of triphos (indeed, C_1–H bond activation has not been seen even for DBT [20]). Of the remaining two activable C–H bonds, the C_2–H one is electronically more deactivated toward metal insertion than the C_3–H bond by the sulfur atom, which disfavors nucleophilic substitutions at the *para* position in DBT [41]. Accordingly, the activation energy for the C_3–H scission is expected to be lower than that for the C_2–H scission, and the corresponding 3-Me_2DBTyl product (**6**) would form more rapidly than the 2-Me_2DBTyl product (**7**). On the other hand, the former compound appears more destabilized than the latter by the steric interaction between the Me_2DBTyl ligand and the phenyl substituents on the basal P atoms of triphos. As a result, the 2-Me_2DBTyl complex should be thermodynamically favored over the 3-Me_2DBTyl isomer. Indeed, we observe that **6** thermally converts to **7**. At 90 °C, this transformation is quite fast but not selective as the (tetrahydrofuranyl)dihydride complex [(triphos)Ir(H)$_2$(C_4H_7O)] (**8**) is also formed by C–H bond activation of THF. The concentration of **8** increases with time at the expense of those of **6** and **7** (after 7 h at 90 °C, the **6**:**7**:**8** ratio is 8:21:71) (Scheme 6). Heating to 120 °C results in the disappearance of the Me_2DBT C–H insertion product and in the exclusive formation of the THF C–H activation products.

In conclusion, only C–H bond activation of either Me_2DBT or THF is brought about by [(triphos)IrH] in the temperature range from 70 to 120 °C with kinetic preference for the cleavage of the sp^2-hybridized C–H bond of Me_2DBT over the sp^3-hybridized C–H bond of THF. The major thermodynamic stability of the THF activation product is surprising [42], but can be rationalized on the basis of steric considerations. For example, [Fe(dmpe)$_2$] [43] (dmpe = 1,2-dimethylphosphinoethane) and [(C_5Me_5)Rh(PMe_3)] [44] react with toluene showing thermodynamic preference for the *meta* and *para* C–H activation of the phenyl ring. Trace amounts of a benzylic C–H activation product (< 1%) were observed in the case of the Rh system at low temperature, but not under conditions of thermodynamic control, however [44]. On the other hand, selective benzylic C–H activation was observed in the reaction of transient [(C_5H_5)$_2$W] with *p*-xylene and mesitylene, and was attributed to the prevalence of steric effects over electronic effects [45] (metal–aryl bonds are generally stronger than metal–alkyl bonds [46]). A similar argument may be invoked to explain the observed thermodynamically favored C–H activation of THF by [(triphos)IrH]. This fragment is more sterically demanding than [(C_5Me_5)Rh(PMe_3)]; the thermodynamic preference of the iridium fragment for sp^3-hybridized C–H bond activation over sp^2-hybridized C–H bond activation may thus be sterically driven as the tetrahydrofuranyl ligand is smaller than the 4,6-dibenzothienyl ligand.

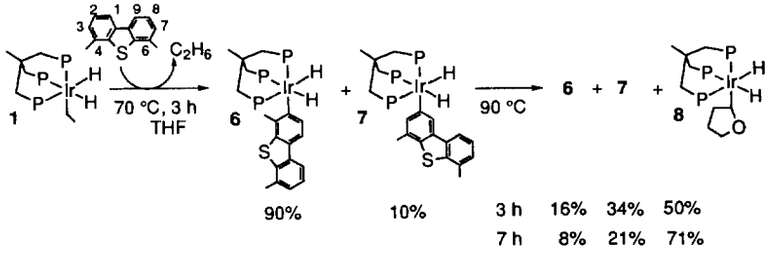

Scheme 6.

4. Conclusions

Excellent thermal stability and great basicity of the metal center are the characteristics which allow the highly energetic fragment [(triphos)IrH] to oxidatively cleave either C–H or C–S bonds from encumbered thiophenes such as 2-methylbenzo[*b*]thiophene, 2,5-dimethylthiophene and 4,6-dimethyldibenzo[*b*,*d*]thiophene. The energy barrier to C–S insertion is higher than that to C–H insertion for Me_2T, whilst it is of comparable entity for MeBT. In both cases, however, the methyl substituents enhance the energy barrier to C–S insertion (Me_2T > MeBT) as compared to the unsubstituted parent thiophenes [18,27]. Two methyl substituents in the 4- and 6-positions of Me_2DBT, sterically disfavoring η^1-*S*-coordination, prevent the C–S bond cleavage by iridium [9].

The reactivity scheme reported in this paper is qualitatively similar to the trend observed for the HDS of thiophenic molecules over heterogeneous catalysts [36] and confirms that C–S insertion is the key step to consider for developing a new generation of more efficient catalysts for deep HDS processes [47].

Acknowledgements

Thanks are due to the EC (contract ERB CHRX CT 930147) and to the Progetto Strategico "Tecnologie Chimiche Innovative", CNR, Rome, Italy for financial support.

References

[1] T. Kabe, A. Ishihara, H. Tajima, Ind. Eng. Chem. Res. 31 (1992) 1577; G.D. Galpern, in S. Gronowitz (Ed.), Chemistry of Heterocyclic Compounds, vol. 44, Part 1, Wiley, New York, 1986, p 325; C. Willey, M. Iwao, R.N. Castle, M.L. Lee, Anal. Chem. 53 (1981) 400.
[2] C. Bianchini, A. Meli, J. Chem. Soc., Dalton Trans. (1996) 801; R.J. Angelici, Bull. Soc. Chim. Belg. 104 (1995) 265; in R.B. King (Ed.) Encyclopedia of Inorganic Chemistry, vol. 3, Wiley, New York, 1994, p. 1433; R.A. Sánchez-Delgado, J. Mol. Catal. 86 (1994) 287; T.B. Rauchfuss, Progr. Inorg. Chem. 39 (1991) 259; R.J. Angelici, Coord. Chem. Rev. 105 (1990) 61; Acc. Chem. Res. 21 (1988) 387; C. Bianchini, A. Meli, in B. Cornils, W.A. Herrmann (Eds.), Applied Homogeneous Catalysis with Organometallic Complexes, vol. 2, VCH, Weinheim, 1996, p. 969.
[3] C. Bianchini, J.A. Casares, A. Meli, F. Vizza, R.A. Sánchez-Delgado, Polyhedron (1997), in press.
[4] C. Bianchini, M.V. Jiménez, A. Meli, F. Vizza, Organometallics 14 (1995) 4858.
[5] I.E. Buys, L.D. Field, T.W. Hambley, A.E.D. McQueen, J. Chem. Soc., Chem. Commun. (1994) 557.
[6] L. Dong, S.B. Duckett, K.F. Ohman, W.D. Jones, J. Am. Chem. Soc. 114 (1992) 151.
[7] W.D. Jones, L. Dong, J. Am. Chem. Soc. 113 (1991) 559.
[8] A.W. Myers, W.D. Jones, S.M. McClements, J. Am. Chem. Soc. 117 (1995) 11704.
[9] A.W. Myers, W.D. Jones, Organometallics 15 (1996) 2905.
[10] A.E. Ogilvy, M. Draganjac, T.B. Rauchfuss, S.R. Wilson, Organometallics 7 (1988) 1171.
[11] Q. Feng, T.B. Rauchfuss, S.R. Wilson, Organometallics 14 (1995) 2923; S.C. Huckett, L.L. Miller, R.A. Jacobson, R.J. Angelici, Organometallics 7 (1988) 686; J. Chen, L.M. Daniels, R.J. Angelici, J. Am. Chem. Soc. 112 (1990) 199.
[12] H. Krautscheid, Q. Feng, T.B. Rauchfuss, Organometallics 12 (1993) 3273.
[13] A.E. Skaugset, T.B. Rauchfuss, S.R. Wilson, J. Am. Chem. Soc. 114 (1992) 8521.
[14] K.M. Dailey, T.B. Rauchfuss, A.L. Rheingold, G.P.A. Yap, J. Am. Chem. Soc. 117 (1995) 6396; S. Luo, T.B. Rauchfuss, Z. Gan, J. Am. Chem. Soc. 115 (1993) 4943.
[15] S. Luo, A.E. Ogilvy, T.B. Rauchfuss, A.L. Rheingold, S.R. Wilson, Organometallics 10 (1991) 1002.
[16] C. Bianchini, A. Meli, M. Peruzzini, F. Vizza, F. Zanobini, Coord. Chem. Rev. 120 (1992) 193; H.A. Mayer, W.C. Kaska, Chem. Rev. 94 (1994) 1239.
[17] C. Bianchini, M.V. Jiménez, A. Meli, S. Moneti, F. Vizza, J. Organomet. Chem. 504 (1995) 27.
[18] C. Bianchini, P. Frediani, V. Herrera, M.V. Jiménez, A. Meli, L. Rincón, R.A. Sánchez-Delgado, F. Vizza, J. Am. Chem. Soc. 117 (1995) 4333.
[19] C. Bianchini, A. Meli, M. Peruzzini, F. Vizza, S. Moneti, V. Herrera, R.A. Sánchez-Delgado, J. Am. Chem. Soc. 116 (1994) 4370.
[20] C. Bianchini, M.V. Jiménez, A. Meli, S. Moneti, F. Vizza, V. Herrera, R.A. Sánchez-Delgado, Organometallics 14 (1995) 2342.
[21] C. Bianchini, D. Fabbri, S. Gladiali, A. Meli, W. Pohl, F. Vizza, Organometallics, 15 (1996) 4604.
[22] C. Bianchini, V. Herrera, M.V. Jiménez, A. Meli, R.A. Sánchez-Delgado, F. Vizza, J. Am. Chem. Soc. 117 (1995) 8567.
[23] R. Gerdil, E.A. Lueken, J. Am. Chem. Soc. 87 (1965) 213.
[24] P.L. Barbaro, C. Bianchini, A. Meli, M. Peruzzini, A. Vacca, F. Vizza, Organometallics 10 (1991) 2227.
[25] J. Jeener, O.H. Meier, P. Bachmann, R. Ernst, J. Chem. Phys. 71 (1979) 4545.
[26] V. Sklener, H. Zon, O. Miyashiro, H.T. Miles, A. Bax, FEBS Lett. 208 (1986) 94.
[27] C. Bianchini, A. Meli, M. Peruzzini, F. Vizza, P. Frediani, V. Herrera, R.A. Sánchez-Delgado, J. Am. Chem. Soc. 115 (1993) 2731.
[28] P. Janser, L.M. Venanzi, F. Bachechi, J. Organomet. Chem. 296 (1985) 229.
[29] C. Bianchini, P.L. Barbaro, A. Meli, M. Peruzzini, A. Vacca, F. Vizza, Organometallics 12 (1993) 2505.
[30] D.T. Cromer, J.T. Waber, Acta Crystallogr. 18 (1965) 104.
[31] International Tables of Crystallography, vol. 4, Kynoch Press, Birmingham, UK, 1974.
[32] N. Walker, D. Stuart, Acta Crystallogr. A39 (1983) 158.
[33] G.M. Sheldrick, SHELXL-93, Program for Structure Determination, University of Göttingen, Germany, 1994.
[34] A. Altomare, M.C. Burla, M. Camalli, G. Cascarano, C. Giacovazzo, A. Guagliardi, G. Polidori, J. Appl. Crystallogr. 27 (1994) 435.
[35] D.A. Lesch, J.W. Richardson Jr., R.A. Jacobson, R.J. Angelici, J. Am. Chem. Soc. 106 (1984) 2901.
[36] B.C. Gates, Catalytic Chemistry, Wiley, New York, 1992, chapter 5, p. 390; B.C. Wiegand, C.M. Friend, Chem. Rev. 92 (1992) 491; M.J. Girgis, B.C. Gates, Ind. Eng. Chem. Res. 30 (1991) 2021; R. Prins, V.H.J. deBeer, G.A. Somorjai, Catal. Rev.-Sci. Eng. 31 (1989) 1; C.M. Friend, J.T. Roberts, Acc. Chem. Res. 21 (1988) 394.

[37] J.W. Benson, R.J. Angelici, Organometallics 12 (1993) 680; 11 (1992) 922.
[38] M.L. Spera, W.D. Harman, Organometallics 14 (1995) 1559; R. Cordone, W.D. Harman, H. Taube, J. Am. Chem. Soc. 111 (1989) 5969.
[39] W.D. Jones, R.M. Chin, J. Organomet. Chem. 472 (1994) 311; J. Am. Chem. Soc. 114 (1992) 9851.
[40] J.J. Garcia, B.E. Mann, H. Adams, N.A. Bailey, P.M. Maitlis, J. Am. Chem. Soc. 117 (1995) 2179.
[41] H. Gilman, A.L. Jacoby, J. Org. Chem. 3 (1938) 108 and references cited therein.
[42] J.P. Collman, L.S. Hegedus, Principles and Applications of Organotransition Metal Chemistry, University Science Books, Mill Valley, CA, 1987.
[43] C.A. Tolman, S.D. Ittel, A.D. English, J.P. Jesson, J. Am. Chem. Soc. 101 (1979) 1742.
[44] W.D. Jones, F.J. Feher, J. Am. Chem. Soc. 106 (1984) 1650.
[45] K. Elmitt, M.L.H. Green, R.A. Forder, I. Jefferson, K. Prout, J. Chem. Soc., Chem. Commun. (1974) 747.
[46] W.D. Jones, F.J. Feher, Acc. Chem. Res. 22 (1989) 91.
[47] R. Navarro, B. Pawelec, J.L.G. Fierro, P.T. Vasudevan, J.F. Cambra, P.L. Arias, Appl. Catal. A 137 (1996) 269; D. Yitzhaki, M.V. Landau, D. Berger, M. Herskowitz, Appl. Catal. A 122 (1995) 99.